Planta (2011) 234:157–169
DOI 10.1007/s00425-011-1394-z

ORIGINAL ARTICLE

Down-regulation of the *myo*-inositol oxygenase gene family has no effect on cell wall composition in Arabidopsis

Stefanie Endres · Raimund Tenhaken

Received: 7 October 2010 / Accepted: 24 February 2011 / Published online: 11 March 2011

Abstract The enzyme *myo*-inositol oxygenase (MIOX; E.C. 1.13.99.1) catalyzes the ring-opening four-electron oxidation of *myo*-inositol into glucuronic acid, which is subsequently activated to UDP-glucuronic acid (UDP-GlcA) and serves as a precursor for plant cell wall polysaccharides. Starting from single T-DNA insertion lines in different *MIOX*-genes a quadruple knockdown (*miox1/2/4/5*-mutant) was obtained by crossing, which exhibits greater than 90% down-regulation of all four functional *MIOX* genes. *Miox1/2/4/5*-mutant shows no visible phenotype and produces viable pollen. The alternative pathway to UDP-glucuronic acid via UDP-glucose is upregulated in the *miox1/2/4/5*-mutant as a compensatory mechanism. *Miox1/2/4/5*-mutant is impaired in the utilization of *myo*-inositol for seedling growth. The incorporation of *myo*-inositol derived sugars into cell walls is strongly (>90%) inhibited. Instead, *myo*-inositol and metabolites produced from *myo*-inositol such as galactinol accumulate in the *miox1/2/4/5*-mutant. The increase in galactinol and raffinose family oligosaccharides does not enhance stress tolerance. The ascorbic acid levels are the same in mutant and wild type plants.

Keywords Cell wall precursors · Functional genomics · Inositol metabolism · *Myo*-inositol oxygenase · Nucleotide sugar biosynthesis · Raffinose family oligosaccharides

Electronic supplementary material The online version of this article (doi:10.1007/s00425-011-1394-z) contains supplementary material, which is available to authorized users.

S. Endres · R. Tenhaken (✉)
Department of Cell Biology, Plant Physiology, University of Salzburg, Hellbrunnerstr. 34, 5020 Salzburg, Austria
e-mail: raimund.tenhaken@sbg.ac.at

Abbreviations

GlcA	D-glucuronic acid
MIOX	*Myo*-inositol oxygenase
miox1/2/4/5-mutant	Quadruple knockdown in all four *MIOX* genes
UDP-GlcA	UDP-D-glucuronic acid
UGD	UDP-glucose dehydrogenase

Introduction

The plant cell wall is the world's most abundant organic resource. Its most obvious function is morphology: it counteracts turgor pressure, forming, shaping and directing growth of the plant on a cellular level as well as the whole individual. Much of the cell wall biomass is derived from a common but cell wall-specific biochemical precursor, UDP-glucuronic acid (UDP-GlcA). In the model plant *Arabidopsis thaliana* about 50% of the cell wall biomass of mature leaves is derived from UDP-GlcA (Zablackis et al. 1995). The wood of many trees contains large amounts of hemicelluloses, in particular xylan, which is largely derived from UDP-GlcA. Given this importance, the biosynthesis of UDP-GlcA attracts our interest. As initially reported half a century ago, plants have established two pathways for the biosynthesis of UDP-GlcA (compare Fig. 1). It can be directly formed from UDP-glucose by the enzyme UDP-glucose dehydrogenase (UGD). This activity is encoded by a small gene family in Arabidopsis (Klinghammer and Tenhaken 2007). The second pathway starts with the biosynthesis of *myo*-inositol, which is subsequently converted to glucuronic acid by a unique type of oxygenase: *myo*-inositol oxygenase (MIOX; E.C. 1.13.99.1). The product

requires the activity of glucuronokinase (Pieslinger et al. 2010) and a UDP-sugar pyrophosphorylase (Kotake et al. 2004) to finally end up in the pool of UDP-GlcA. The functionality of the MIOX pathway for plant cell wall biosynthesis has been shown in the past (Kroh and Loewus 1968; Wakabayashi et al. 1989; Loewus and Murthy 2000). After purification of the MIOX enzyme from *Cryptococcus* (Kanter et al. 2003), we cloned and characterized the corresponding Arabidopsis gene family for *MIOX* which has four active members.

Exploring public microarray databases (http://www.genevestigator.com) and *MIOX-promoter::GUS* lines (Kanter et al. 2005), we found a strong developmentally regulated gene expression of the different *MIOX* isoforms. Two developmental stages, young seedlings and flowers, in particular anthers and pollen, show the highest expression levels for *MIOX* genes. The role of the MIOX pathway to UDP-GlcA in Arabidopsis cell cultures has been addressed by Sharples and Fry (2007) by feeding radioactive precursors. They found a predominant role of UDP-glucose dehydrogenase for this type of tissue. However, these feeding studies are not feasible for all types of differentiated plant tissues.

MIOX genes can be found in almost all eukaryotes but are generally absent in prokaryotes. One of the few exceptions is the cyanobacteria *Nostoc punctiforme*, which has a single predicted *MIOX* gene based on bioinformatic homology searches. The amino acid sequences are highly conserved between species even from different phyla indicating a common evolutionary origin.

The MIOX protein from mouse was recently crystallized to get deeper insight into structure and enzymatic mechanism. The di-iron centre is coordinated by two His-residues for each of the two iron atoms which are additionally bridged by a water and an aspartate molecule (Brown et al. 2006). MIOX was found to have a valence-localized Fe(II)/Fe(III) pair as catalytically competent state, which sets it apart from other oxygenases. The catalytic cycle is unique in that it performs a full four-iron oxidation of the substrate, returning to its resting state without need for an external reductant (Moskala et al. 1981; Xing et al. 2006a, b, c). The terminal electron acceptor is oxygen, which is converted to water.

Myo-inositol is used by plant cells to synthesize a variety of low molecular weight compounds. Phytic acid, the hexakisphosphate ester of *myo*-inositol, accumulates in seeds as the major phosphor storage compound (Raboy 2001). Inositol also serves as a substrate for the formation of galactinol, the galactosyl-donor that plays a key role in the formation of raffinose family oligosaccharides (RFOs, raffinose, stachyose, verbascose) from sucrose. RFOs accumulate in plants under various stress conditions (Blackman et al. 1992; Kaplan et al. 2004; Peters et al. 2007).

Here we investigate the role of the MIOX enzyme family in knockout/knockdown mutant. To reduce the

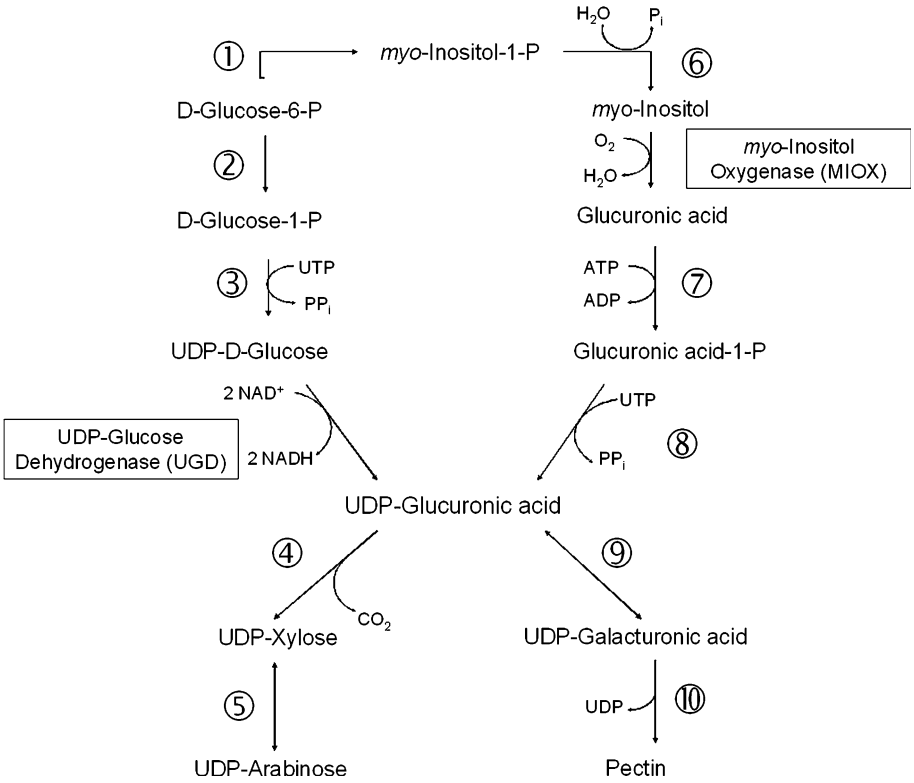

Fig. 1 Biosynthesis of UDP-glucuronic acid and related cell-wall precursors. Two branches lead to the cell wall precursor UDP-glucuronic acid: the *myo*-inositol oxygenation pathway with MIOX activity as committing step (*right*), and the nucleotide sugar oxidation pathway depending on UGD activity (*left*) (Seifert 2004; Kanter et al. 2005; Reiter 2008). ① Inositol-1-P-synthase; ② Phosphoglucomutase; ③ UDP-glucose pyrophosphorylase; ④ UDP-glucuronic acid decarboxylase; ⑤ UDP-arabinose 4-epimerase; ⑥ Inositolphosphate-phosphatase; ⑦ Glucuronokinase; ⑧ UDP-sugar pyrophosphorylase; ⑨ UDP-glucuronic acid 4-epimerase; ⑩ α-Galacturonosyl transferase

genetic redundancy of the pathway we have crossed single T-DNA insertion lines for each isoform to double, triple and finally a quadruple knockdown mutant hereafter referred to as the *miox1/2/4/5*-mutant. This allows the analysis of the function of this enzyme as the activity is strongly reduced or almost absent in the mutant depending on the tissue under investigation. One of the original questions was the contribution of the MIOX pathway to cell wall biosynthesis in plants and whether the enzyme UDP-glucose dehydrogenase could compensate for a loss in MIOX. We assume from our experiments that the latter assumption of complementation by UGD is correct.

Materials and methods

Plant growth

Plants were grown in standard fertilized soil (ED73; Einheitserde; www.einheitserde.de) in a growth chamber (23°C; 150 µmol photons m^{-2} s^{-1}). *Arabidopsis thaliana* seeds Col (cultivar Columbia; NASC, University of Nottingham, UK, stock no. N60000) and the *vtc1*-mutant were obtained from the NASC stock centre. The *MIOX* quadruple knockdown mutant *miox1/2/4/5* was produced from cross-fertilization of the four T-DNA-insertion lines Gabi 450D10 (*miox1*), Salk 040608 (*miox2*), Salk 018395 (*miox4*) and Salk 112535 (*miox5*). First, two double mutants *miox1/2* and *miox4/5* were isolated and genotyped to isolate a homozygous lines (Siddique et al. 2009). The *miox1/2* mutant was crossed with a homozygous *miox4*-mutant and homozygous triple mutants *miox1,2,4* were isolated. The *miox4,5* mutant was crossed with a homozygous *miox2* line, selfed, and homozygous triple mutants *miox2,4,5* were identified. Both triple mutants *miox1/2/4* and *miox2,4,5* were finally crossed, selfed, and siblings were characterized by PCR for homozygous T-DNA insertion in all four *MIOX* genes, resulting in the quadruple mutant *miox1,2,4,5*.

The *CaMV35S::MIOX4* lines were kindly provided by the Nessler group (Department of Plant Pathology, Virginia Tech, Blacksburg, VA, USA) and are described in Lorence et al. (2004). The *pgm* mutant was a kind gift from Mark Stitt (Max Planck Institute for Molecular Plant Physiology, Golm, Germany).

PCR techniques

DNA was extracted from young leaves and the genetic identity of the plants determined by PCR technique. The mixture was supplemented with 0.6 M betaine (final concentration), otherwise only faint product bands were observed. The thermal profile was as follows: 92°C, 3 min; 32 × [92°C, 15 s; 58°C, 30 s; 72°C, 1 min]; 72°C, 3 min. The primers are given in Suppl. Table S1. T-DNA insertion sites were determined from PCR fragments spanning the insertion site. They were subcloned into pJET 1.2, amplified and sequenced for exact determination of the insertion site.

Quantitative PCR

RNA from different tissues was extracted with the NucleoSpin RNA Plant kit (Macherey-Nagel) and transcribed to cDNA using the RevertAid Moloney murine leukaemia virus reverse transcriptase kit (Fermentas).

For quantification of *MIOX* and *UGD* transcripts, qPCR was performed on a Stratagene MX3000 realtime cycler using a SybrGreen method. One reaction (30 µL) consisted of 1× PCR-buffer, a 1:200,000 dilution of SybrGreen stock (Roche), 200 nM primers each, and 1 U Taq polymerase (recombinant wild type). Primers are given in Suppl. Table S2. For amplification of *MIOX* transcripts, we added betaine to a final concentration of 0.6 M. The housekeeping gene *EF1α* was employed for internal correction.

The qPCR programme for *MIOX* cycles through 30 s at 92°C, 30 s at 59°C, and 15 s at 72°C for 40 times; the one for *UGD* through 30 s at 94°C, 20 s at 58°C, and 30 s at 72°C for 40 times; a conclusive melting curve indicates identity and homogeneity of the product.

For calculations, the reaction efficiencies of the individual wells were computed from the original data employing the LinRegPCR software version 7.4 and raised to the power of the corresponding threshold cycle value. Results were averaged over triplicates and normalized with the calculated amounts of *EF1α* transcripts.

Feeding of *myo*-inositol/labelling with ^{3}H-*myo*-inositol: incorporation in seedlings

Surface-sterilized seedlings were suspended in 0.5 mL one-half-strength Murashige and Skoog medium with 2.5 mM Mes (adjusted to pH 5.6 with KOH), 0.1% sucrose, and 1 µM *myo*-[2-^{3}H]inositol (specific activity 555 GBq $mMol^{-1}$; Amersham/GE Healthcare). After 7 days, 25 seedlings (approx. 50 mg fresh weight) were rinsed first in 1 g L^{-1} inositol, then in water, carefully rid of their seed coats, blotted dry and frozen in liquid nitrogen. The samples were homogenized in a Retsch ball mill and subsequently resolved in 200 µL 0.2 M Na_2HPO_4, pH 7.4. This crude extract was split into pellet and supernatant by centrifugation (18,000*g*, 10 min); the pellet was washed several times according to Kanter et al. (2005) to obtain the "cell wall" fraction. The supernatant was mixed with 800 µL acetone and incubated over night at −20°C. Centrifugation for 15 min at 4°C resulted in a supernatant

retaining soluble sugars while oligosaccharides and proteins precipitated. The pellet was further treated with α-amylase (Sigma A6380) and amyloglucosidase (Sigma A1602) to degrade starch from the pellet and solubilize glucose units. The enzymes are essentially free of other carbohydrate hydrolases.

Feeding of *myo*-inositol/labelling with ^{3}H-*myo*-inositol: incorporation in leaf discs

Leaf discs of 8 mm in diameter were cut out of fully expanded leaves and immediately floated abaxial side down on inositol-free Murashige and Skoog medium (compare Endres and Tenhaken 2009) with 2.5 mM Mes buffered at pH 5.6 (KOH). *myo*-[2-^{3}H]Inositol (specific activity 555 GBq mMol^{-1}; Amersham/GE Healthcare) and unlabelled *myo*-inositol were added to a final concentration of 1 and 500 µM, respectively. After 3 h of incubation at room temperature and low light conditions, the discs were rinsed in water, blotted dry, and processed.

When feeding cold inositol, the final concentration of this compound was 1 g L^{-1} (ten times more than in regular Murashige and Skoog media). After allowing the leaf discs to take up inositol at room temperature and low light conditions for 2 h, they were carefully rinsed in pure water, blotted on filter paper, and transferred to inositol-free medium. Samples were measured at appropriate time points. Control samples were kept in inositol-free medium over the time course of the experiment. Samples were resuspended in Rotiszint eco plus cocktail (Roth) and counted in a Liquid Scintillation Analyzer TRI-CARB 2100TR (Packard).

Fractionation of labelled material

Monosaccharides from the TFA hydrolysate from seedlings grown in liquid one-half-strength MS supplied with ^{3}H-*myo*-inositol were analyzed on a high performance anion exchange chromatography with pulsed amperometric dectection (HPAEC-PAD) using a Dionex ICS 3000 system, equipped with a CarboPac PA-20 column. The separation method is based on Dionex technical note 20 (http://www.dionex.com/en-us/webdocs/5023-TN20.pdf) with the following modifications: Buffer A, 200 mM NaOH; buffer B, 15 mM NaOH; buffer C, 50 mM NaOH with 500 mM sodium acetate; buffer D, 2 mM NaOH. All sugars (except xylose and mannose) were separated under the following conditions: flow rate 0.45 mL min^{-1}; t0 to t15 100%B, t15 to t25 40%C, 60% B; t25-t28 100%B. The column was regenerated with 100%A for 10 min followed by equilibration with starting buffer B. Simultaneously, fractions were collected every 20 s (~150 µL) and scintillation counted. Xylose and mannose were separated in a separate run using buffer D. Quantification of the sugar signal was done with the Chromeleon software using standard curves (0.1–1 nMol of each sugar).

Metabolite analysis

Soluble sugar extraction

The extraction of soluble carbohydrates from leaves was performed as described previously (Endres and Tenhaken 2009). Seed sugar extraction followed the protocol given in Bentsink et al. (2000). Separation of the samples on a CarboPac MA1 analytical column (Dionex) allows identification of, *myo*-inositol, and galactinol. For raffinose (and stachyose) measurements, the same samples were loaded on a PA200 column (Dionex). Sucrose was detected on a PA20 column. Concentrations were determined by comparison to authentic standards. Quantification of ascorbic acid and dehydro-ascorbic acid was performed as described previously (Endres and Tenhaken 2009).

The HPLC method for phytic acid extraction described in Talamond et al. (2000) was adapted as follows: 20 mg of seeds was frozen in liquid nitrogen, homogenized in a Retsch ball mill and resuspended in 1 mL 0.5 M HCl. After 10 min incubation at 90°C, the samples were centrifuged for 10 min and 800 µL of the supernatant were transferred to a new tube. Another 114 µL of 7 M HCl were added, the samples were centrifuged for 5 min at 18,000*g*, and 600 µL of the supernatant were evaporated to dryness. The samples were dissolved in 600 µL water and analyzed on an AS11 analytical column (Dionex) by monitoring conductivity with activated suppressor.

Stress induction and ascorbic acid quantification

Plants adapted to low light (25 µmol photons m^{-2} s^{-1}) for 3 days were transferred to high light conditions (250 µmol photons m^{-2} s^{-1}) and the increase in total ascorbic acid content over time was monitored as detailed in Endres and Tenhaken (2009).

Seed mucilage analysis

Dry seeds (10 mg) were incubated in 300 µL 50 mM HCl for 40 min at 80°C. After centrifugation, the supernatant was transferred to a new tube, the pellet extracted with another 50 µL HCl, and the supernatants were pooled. Addition of 15 µL 1 M NaOH partially neutralized the extract prior to precipitation over night at −20°C with 1.2 mL ethanol. The sample was centrifuged for 10 min at 18,000*g*, the supernatant discarded and the pellet dried.

Once the pellet was completely dry, it was hydrolyzed by autoclaving it for 2 h in 250 µL 2 M TFA and 10 µL 0.5% inositol. Once again the sample was dried, re-dissolved in 200 µL water, centrifuged to sediment particles, and prepared for HPLC analysis (see section Feeding of ^{3}H-inositol).

Cell wall samples

Leaf material (100–150 mg) was frozen in liquid nitrogen, homogenized in a Retsch ball mill and suspended in 70% ethanol. Subsequent extractions with methanol/chloroform and acetone as detailed in Kanter et al. (2005) resulted in a cell wall pellet, which was dried and suspended in 800 µL 0.25 M NaAc (pH 4.0) solution. The sample was incubated at 80°C for 20 min, chilled on ice, and adjusted to a pH of 5.0 with 1 M NaOH. An aliquot of 0.01% NaN_3 was added prior to incubation with 0.5 mg α-amylase and 0.5 µl pullulanase (Sigma) at 37°C over night. The following day, the sample was boiled for 10 min in a water bath, centrifuged at 18,000*g* for 5 min, and the supernatant discarded. To remove all residual free sugars, the pellet was washed with 1 mL water for four times. After two more washing steps with acetone, the pellet was dried. The weight of the sample was determined; the hydrolysis in TFA was performed as described above. The dry sample was re-dissolved in 1 mL distilled water per 3 mg of dry sample; 200 µL were diluted with 300 µL water and analyzed via HPLC (see section Feeding of ^{3}H-inositol).

Treatment with methylviologen

Four-week-old plants grown in standard growth conditions were sprayed with 50 µM methylviologen in 0.1% (v/v) Tween 20 and transferred to a growth chamber where they were exposed to ~1,500 µmol photons m^{-2} s^{-1} light intensity at 15°C ambient temperature. PSII activity was monitored with a Mini PAM Chlorophyll Fluorometer (Walz, Effeltrich, Germany).

Freezing tolerance

The freezing experiments were conducted as detailed in Rohde et al. (2004). The method is based on an increased ion-leakage from cold-treated leaves, when cells do not exhibit freezing tolerance. We tested batches of plants grown under standard growth conditions in three independent experiments. The resulting data were combined and subjected to a sigmoidal fit performed by the Origin software 6.0 according to the Boltzmann-model. Details of the method are given in the supplement.

Sequence data

Sequence data from this article can be found in the GenBank/EMBL data libraries under accession numbers NP_172904.2 (*MIOX1*; At1g14520); NM_127538.3 (*MIOX2*; At2g19800), NM_118759.4 (*MIOX4*; At4g26260); NM_125047 (*MIOX5*; At5g56640).

Results

By cross-fertilization of the four T-DNA-insertion lines Gabi 450D10 (*miox1*), Salk 040608 (*miox2*), Salk 018395 (*miox4*) and Salk 112535 (*miox5*) we obtained a *miox1/2/4/5* quadruple mutant. *MIOX3* (At4g26255) is a transcribed but truncated and highly mutated pseudogene. The mRNA sequence has only partial homology to the neighbouring *MIOX4*-gene and contains numerous stop codons in all three reading frames. In the *miox1/2/4/5*-mutant a PCR-product of the predicted size was obtained for all four *MIOX* genes using the left border T-DNA (LB-T-DNA) insertion primer and a suitable *MIOX* isoform specific primer, consistent with the integration of a T-DNA in each *MIOX* gene (Fig. 2a). Homozygosity of the *miox1/2/4/5*-mutant was tested with *MIOX* gene specific primer pairs, spanning each T-DNA insertion site. Absence of the intact wild type genes can be proven for all four gene loci (Fig. 2a).

Transcript profiling

RNA was isolated from wild type and *miox1/2/4/5*-mutant plants to compare the transcript levels of the four *MIOX* genes in both plant lines. Due to the highly transient nature of *MIOX* expression particularly in flowers as seen in GUS reporter gene plants (Kanter et al. 2005), we performed the analysis with different organs. The wild type data correspond well with data available at Genevestigator (http://www.genevestigator.com; data not shown).

In the *miox1/2/4/5*-mutant, we were able to detect transcripts of *MIOX1*, *MIOX4* and *MIOX5*; leaving *MIOX2* as the only isoform that is knocked out while the others are severely reduced in their transcript levels but not completely knocked out (Fig. 2c). Subcloning of the left border T-DNA insertion sites and ensuing sequencing revealed that the insertions are located close to splice sites or, in the case of *MIOX2* and *MIOX4*, even in an intron sequence (see Fig. 2b). For the qPCR experiments (*MIOX1*, *2*, *4*) we used primer pairs spanning the T-DNA insertion sites. The residual transcripts (Fig. 2c) suggest the presence of residual full length mRNAs. Interestingly, we see that in the *miox1/2/4/5*-mutant *MIOX4* is expressed in tissues

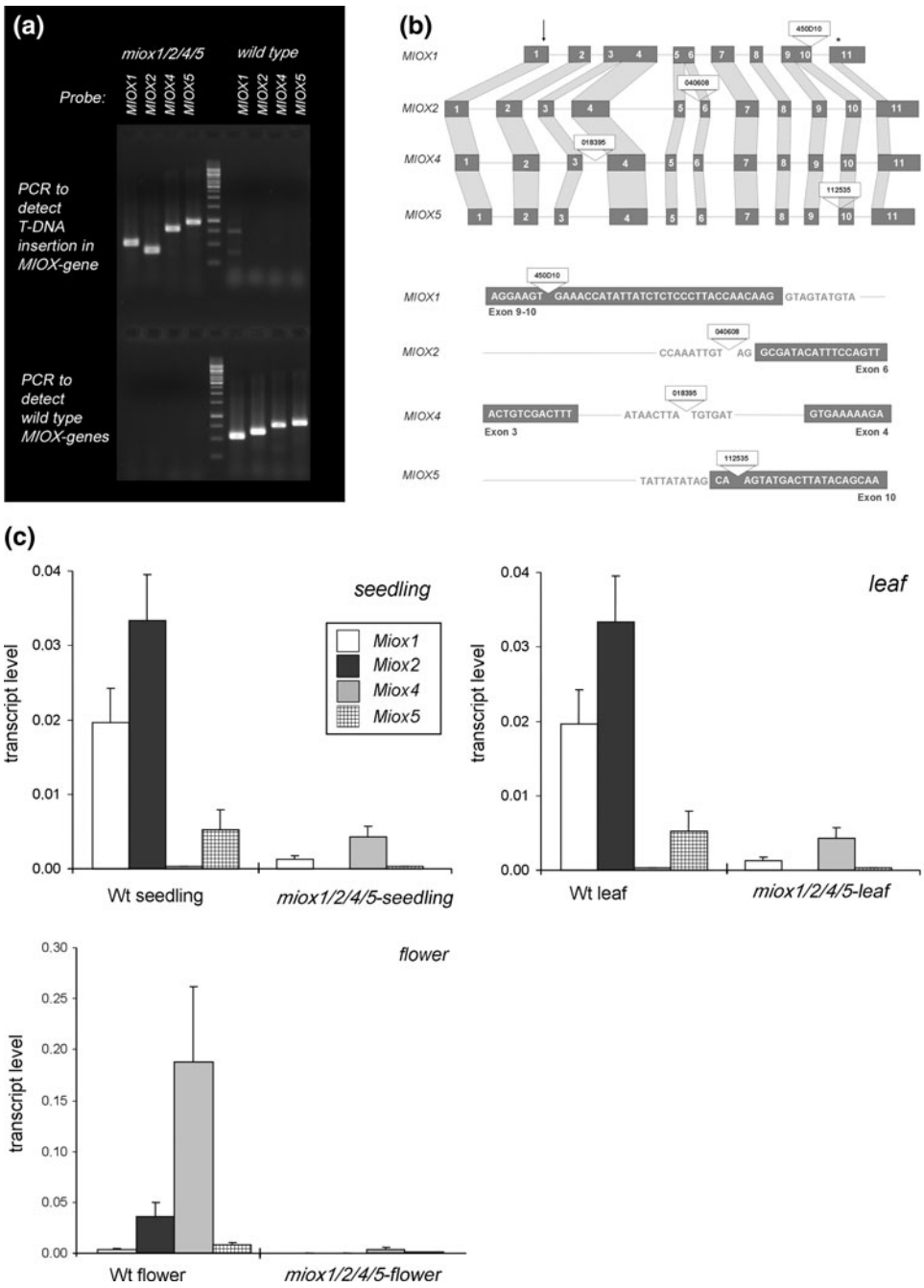

Fig. 2 Genetic characterization of wild type and *miox1/2/4/5*-mutant. **a** Ethidium bromide strained PCR bands verifying the genetic identity of the quadruple knockout in *miox1/2/4/5*. **b** T-DNA insertion sites in the genes of the *MIOX* isoforms. The *upper scheme* shows the relation of *MIOX* isoforms (*grey boxes* exons) and the sites of T-DNA insertions. *MIOX1*: Gabi-Kat, *MIOX2*, *4*, and *5* SALK. The *arrow* indicates the position of the translation start codon, the *asterisks* marks the stop codon. The *lower part* of the illustration shows the exact location of the T-DNA insertion. This information is derived from resequencing the junction site between the *MIOX* gene and the LB of the T-DNA. For *MIOX1*, the insertion site is ~30 bp upstream of a splice site; *MIOX2* and *5* are even closer to splice sites; the SALK lines for *MIOX2* and *MIOX4* are located in an intron; the former again close to a splice site. **c** Expression profile of *MIOX* isoforms. Realtime PCR data of wild type and *miox1/2/4/5*-mutant material are displayed to depict the transcript distribution of *MIOX* relative to a housekeeping gene in three different stages of development: in seedlings, leaves, and in flowers (please note the different scale for flower transcripts indicating the far higher higher expression in this organ). Total relative amounts of transcripts were calculated and the ratio of *miox1/2/4/5*-mutant to wild type was formed. The level of *MIOX* transcripts is highly reduced in *miox1/2/4/5*-mutant. The experiment was performed in triplicates; shown are means and standard deviations

where it is normally not expressed in the wild type (compare Fig. 2c). Still, the total amount of *MIOX* transcripts that can be rescued in the *miox1/2/4/5*-mutant is between 2 (flowers) and 14% (in leaves).

We assumed that a disruption of the MIOX pathway should have consequences for inositol metabolism and cell wall composition. This can be visualized when *miox1/2/4/5*-mutant and wild type plantlets are grown on either inositol-free MS (control) or on medium with 1 g L^{-1} inositol: The lines differ strongly; while the wild type can utilize inositol as additional carbon source and shows increased growth at the same age, *miox1/2/4/5*-mutant seedlings are significantly less developed and resemble the condition without inositol (Fig. 3). A small increase in growth of *miox1/2/4/5*-mutant on *myo*-inositol plates may be caused by the small residual MIOX-activity.

UDP-xylose, UDP-arabinose and UDP-galacturonic acid are derivatives of UDP-glucuronic acid. Therefore, a change in cell wall composition in *miox1/2/4/5* lacking MIOX activity seemed possible. However, HPLC analysis of hydrolyzed cell wall material failed to exhibit the reduction in these sugar residues in *miox1/2/4/5*-mutant cell walls compared to the wild type (Fig. 4a). As the *MIOX* genes are predominantly expressed in flowers and also in developing seeds we also tested the composition of seed coat mucilage, which also shows no significantly altered sugar composition (Fig. 4b).

Inositol feeding experiments in leaf discs

Experiments with leaf discs floating on inositol-enriched medium document rapid uptake of free inositol as described by Schneider et al. (2006). During the feeding situation, the *miox1/2/4/5*-mutant accumulated more free inositol after 2 h of feeding than the wild type (data not shown). The inositol concentration in both lines rapidly dropped down after the feeding of inositol was stopped.

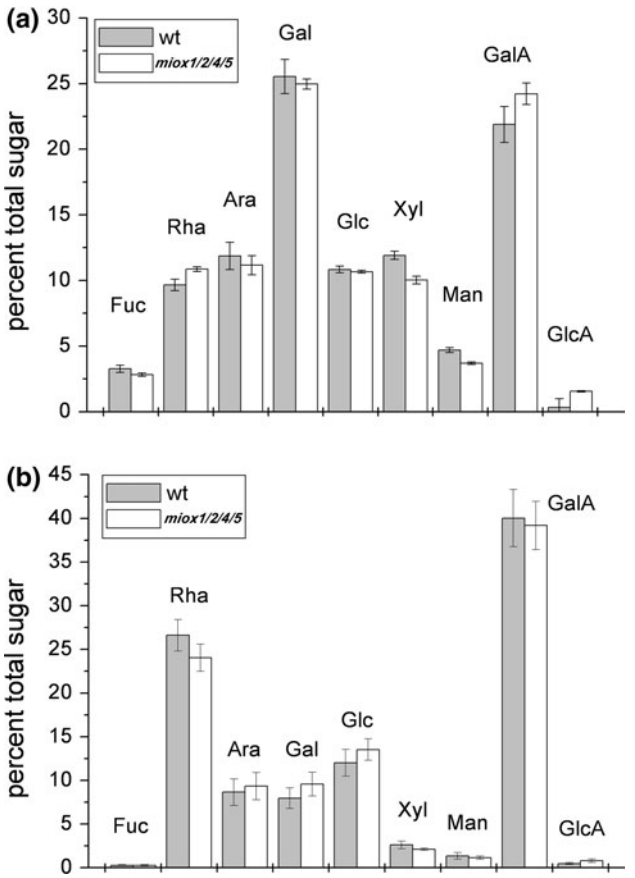

Fig. 4 Sugar composition for cell wall (**a**) and seed mucilage (**b**). Even though MIOX activity is related to cell wall biosynthesis, composition of cell wall and seed mucilage in *miox1/2/4/5*-mutant does not deviate significantly from the wild type. Shown are means and standard deviations of four replicates

To be able to follow the fed inositol, we performed a similar feeding experiment with [^{3}H]-inositol. Figure 5a shows that while all plant lines take up roughly the same total amount of label, wild type and L2 (*CaMV35S::MIOX4* overexpressor line L2; Lorence et al. 2004)

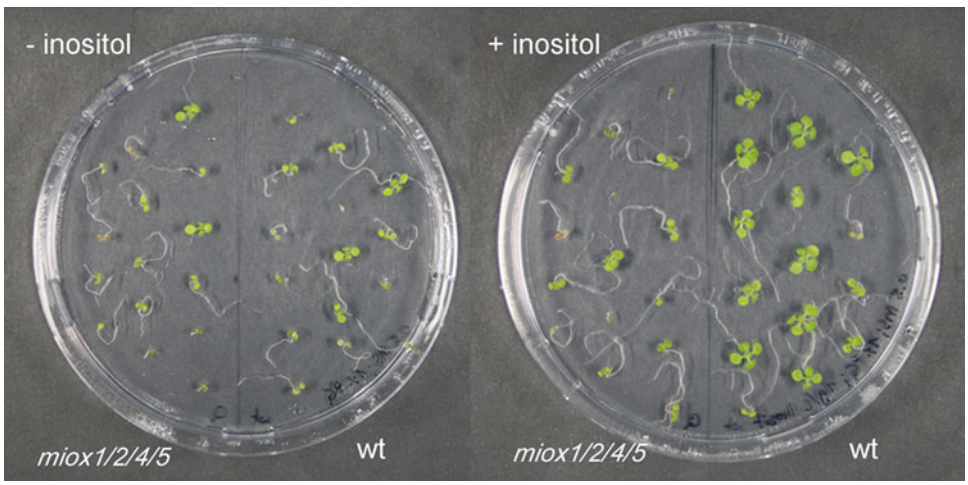

Fig. 3 Utilization of inositol. Wild type seedlings can utilize inositol as additional carbon source for growth, *miox1/2/4/5*-mutant seedlings cannot. Wt seeds on the right side of each dish, *miox1/2/4/5*-mutant seeds on the left side. *Left* inositol-free MS medium, *right* MS medium supplied with 1 g L^{-1} inositol

incorporate approximately 40% of it into the cell wall; in *miox1/2/4/5*-mutant the majority (~95%)of the ^{3}H-label remains in the soluble fraction. We tried to further analyze the signal present in the aqueous phase: by evaporation experiments we were able to exclude the possibility of $^{3}H_2O$ as the source for the label. Incubation with anion or cation exchange beads (Bio-Rex MSZ 501(D) resin, Bio-rad), respectively, showed that no radioactive metabolite bound to the ion-exchange resin, which indicates that the fed [^{3}H]-inositol is not present in a free ionic form. This suggests low amounts of inositol-phosphates in the aqueous phase under these conditions, which were not detectable under our conditions. Extraction with chloroform indicated that a small fraction of the total incorporated label is present in a hydrophobic form in all plant lines tested without showing quantitative differences (data not shown).

Inositol feeding experiments in seedlings

To clarify the identity of the soluble label and the residual signal in the *miox1/2/4/5*-mutant cell wall fraction, we grew seedlings on medium with [^{3}H]-inositol. The distribution of ^{3}H-label between the soluble and insoluble fraction is shown in Fig. 5b. We included a second fractionation step of the aqueous supernatant, a precipitation with 80% acetone, to separate soluble inositol from precipitable galactinol. HPLC analysis confirmed that the radioactive signal in soluble fraction is attributed to inositol and galactinol (data not shown).

Next, we turned our attention to the cell wall fraction. To exclude the possibility of starch as signal source, we performed a digestion with α-amylase and amyloglucosidase. This procedure released roughly one-fifth of the signal from the insoluble fraction, but this observation was made in wild type as well as *miox1/2/4/5*-mutant samples. The necessary incubation in slightly acid buffer also releases part of the pectic fraction and possibly also some arabinogalactan proteins. TFA hydrolysis of the cell wall fraction was performed to investigate whether the pattern of labelled sugars is altered in *miox1/2/4/5*-mutant compared to wild type samples. Figure 6 shows the HPLC elution profile in the upper portion and the scintillation counts of the collected fractions in the lower portion of each graph. Note that the scale for the radioactivity counts (right *Y*-axis) is tenfold lower for the *miox1/2/4/5*-mutant than for the wild type, confirming the >90% reduction of *myo*-inositol conversion into cell wall sugars in the *miox1/2/4/5*-mutant. Signal is found for inositol and the GlcA derivatives GalA, Ara and Xyl. GlcA itself is probably present in too small a concentration to elicit a signal (compare the amount in Fig. 4a). An unidentified signal, presumably resulting from incompletely hydrolyzed sugars, is released from the column during the transition from solely alkaline buffer to a buffer solution that also contains sodium acetate (the corresponding electrochemical signal is seen in the HPLC elution profile as well).

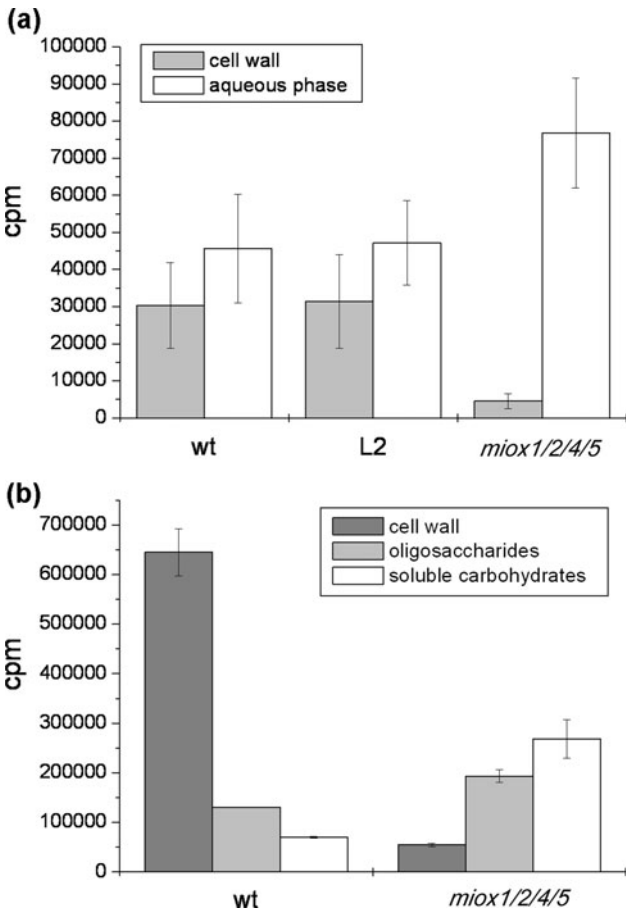

Fig. 5 Incorporation of ^{3}H-*myo*-inositol. **a** Distribution of label during short-term incubation of leaf discs. Leaf discs were floated for 3 h on MS supplemented with ^{3}H-*myo*-inositol and chased for 1 h with cold inositol. The total amount of label found in the three lines is similar. The gain-of-function mutant line L2 expressing a *CaMV35S::MIOX4* construct incorporates slightly more signal into the cell wall than the wild type; the majority of signal detected in the *miox1/2/4/5*-mutant is retained in the soluble fraction. **b** Distribution of label in 7-day-old seedlings. Seedlings were grown in liquid MS supplemented with ^{3}H-*myo*-inositol. The crude extract was split into pellet and supernatant; the pellet was washed several times to obtain the "cell wall" fraction; the supernatant was mixed with acetone to retain soluble sugars in the supernatant while precipitating oligosaccharides. The amount of signal in the cell wall of the *miox1/2/4/5*-mutant is highly reduced compared to the wild type; instead, more signal is found as soluble carbohydrate or acetone precipitate. The experiment was performed in triplicates; shown are means and standard deviations

As we found no changes in the cell wall composition in *miox1/2/4/5*-mutant compared to wild type despite the block via the MIOX enzymes, we measured the transcripts of *UGD*, the key enzyme acting in a parallel reaction pathway leading to UDP-GlcA. UGD-genes are up-regulated (~1.5-fold in seedlings and leaves) in the context of

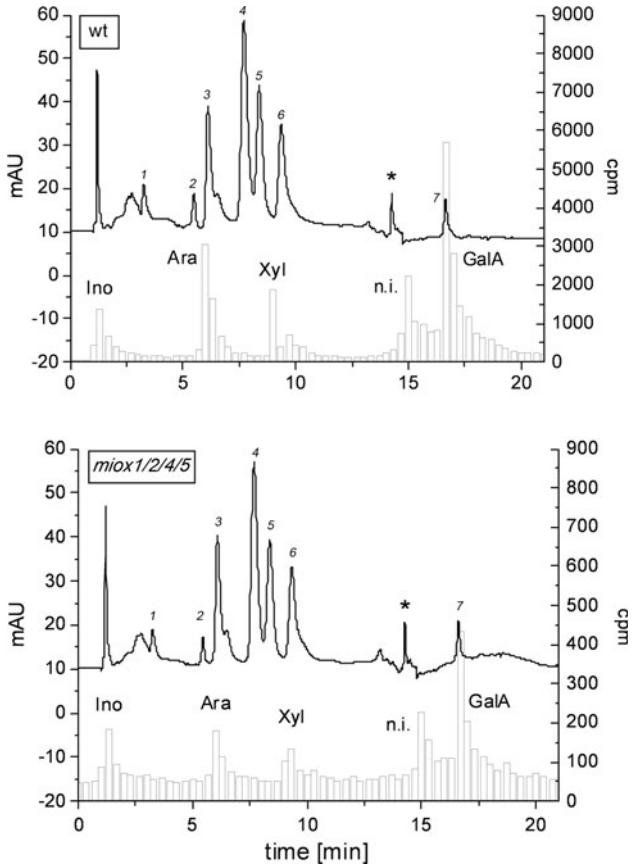

Fig. 6 Distribution of label among cell wall monomers. Labelled cell wall pellets of wild type (*upper panel*) and *miox1/2/4/5*-mutant (*lower panel*) were characterized via HPLC (*line*), fractionated, and scintillation counted (*columns*). *1* Fuc, *2* Rha, *3* Ara, *4* Gal, *5* Glc, *6* Xyl, *7* GalA. *Asterisks* signal from buffer change. Please note the different scale for radioactive metabolites, used for wild type and *miox1/2/4/5*-mutant plants

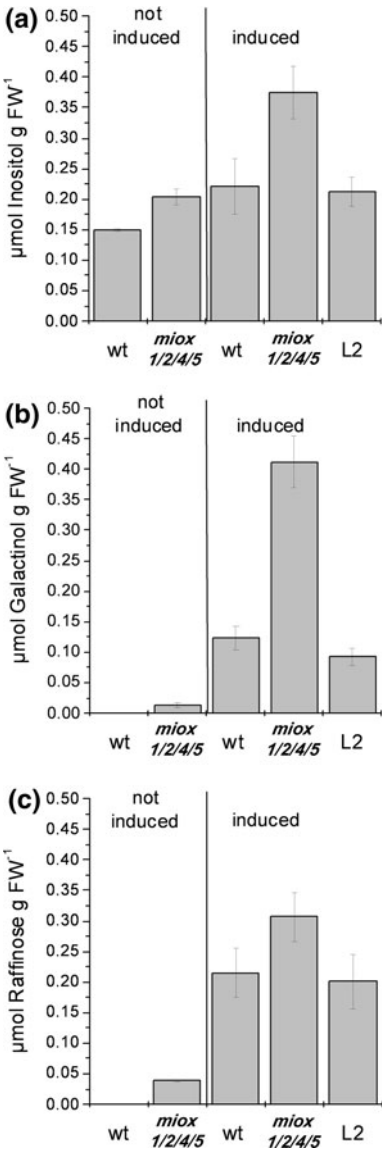

Fig. 7 Salt-stress treatment leads to an increase of inositol and derivatives. Soluble carbohydrates were extracted from young leaves of 6-week-old plants 5 days after watering them with 150 mM NaCl ("induced" samples). Wild type plants, the *miox1/2/4/5-mutant* and a *CaMV35::MIOX4* overexpressor line (L2) are compared. As a control served a set of plants that received tap water instead ("not induced"). Accumulation for inositol (**a**), galactinol (**b**) and raffinose (**c**) is presented. Shown are means and standard deviation of three independent experiments

our *miox1/2/4/5*-mutant—to the greatest extent in the flower ($\sim$3-fold), where the lack of *MIOX* transcript must be most pronounced. The increase in *UGD* transcripts results in approximately 15% higher UGD activity in flowers. The lack of a visible phenotype in the *miox1/2/4/5*-mutant is likely explained by the compensatory effect of increased UGD activity and the residual activity of MIOX in the *miox1/2/4/5*-mutant.

Metabolite profiling

Investigation of the RFOs, biosynthetic pathway is shown in Suppl. Fig. S1, shows an increase in *miox1/2/4/5*-mutant leaves under standard conditions which can even be elicited to a greater extend when salt stress is applied. In L2 (MIOX overexpressor), where the level of free inositol is lower due to increased MIOX activity, the response to salt stress is somewhat weaker than in the wild type (Fig. 7).

In seeds, the changes are displayed even more intensely: approximately 50× more free inositol and 5× more galactinol is present in *miox1/2/4/5*-mutant seeds compared to the wild type. Raffinose content is the same, and stachyose is reduced. We also observed that the content of phytic acid, the inositol-hexakisphosphate which serves as ion chelator and phosphate-storage molecule, is higher in *miox1/2/4/5*-mutant than in wild type or an overexpressing line (Fig. 8a, b).

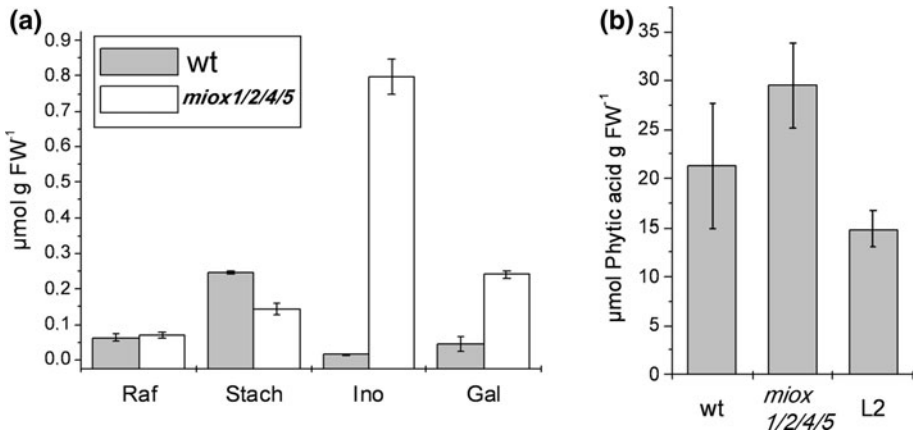

Fig. 8 Seed sugar content. **a** Inositol and RFO content in seeds. The *miox1/2/4/5*-mutant shows highly increased levels of free inositol and the galactosylated inositol galactinol. **b** Phytic acid content in seeds of wild type, *miox1/2/4/5*-mutant and a *CaMV35::MIOX4* overexpressor line (L2). The level of the fully phosphorylated inositol-derivative phytic acid is elevated in *miox1/2/4/5*-mutant and reduced in the *MIOX4*-overexpressing line L2. A *t* test shows significant ($P < 0.05$) differences between samples, despite the large SD. Shown are means and SDs of triplicates

Seedling characterization

Based on these findings, we decided to conduct a series of germination experiments (the data is summed up in Suppl. Fig. S2). First, we measured the inositol content in seedlings grown on media with differing inositol contents. This clearly demonstrated that the *miox1/2/4/5*-mutant plantlets not only accumulate externally applied inositol, but that their intrinsic level of autonomously synthesized inositol is high even at conditions where no free inositol can be detected in the wild type or L2 (MIOX overexpressor). Second, we performed a basic stress treatment with two concentrations of NaCl (50 and 150 mM). *miox1/2/4/5*-mutant is more sensitive than the wild type. This is a bit surprising since inositol and RFOs are interpreted as osmolytes which should convey a greater resistance to such stresses—not the greater susceptibility we see in this experiment. Third, we incubated seeds on phosphate-free MS medium, assuming that the increased level of phytic acid seen in *miox1/2/4/5*-mutant seeds enables them to deal better with this situation. Indeed, we see a slightly higher growth rate in *miox1/2/4/5*-mutant seedlings compared to the wild type.

Adult plant characterization

The RFOs are discussed to be involved in stress tolerance. Nishizawa et al. (2008) found plants with high galactinol and raffinose contents less susceptible to oxidative stress as measured via chlorophyll quenching after treatment with methylviologen. We repeated this experiment with our *miox1/2/4/5*-mutant line, but could not detect a similar protective effect of its elevated galactinol and raffinose content compared to the wild type, neither in standard (not shown) nor in high light conditions (Suppl. Fig. S3a).

Rohde et al. (2004) saw a correlation between high raffinose levels and increased freezing tolerance. We assumed that the elevated level of raffinose even at standard growth conditions might convey a similar freezing tolerance to our *miox1/2/4/5*-mutant plants. However, determination of the percentage of ion leakage did not result in significantly differing values (Suppl. Fig. S3b).

In a third line of experiments, we investigated the correlation of MIOX activity and ascorbic acid content as postulated in Lorence et al. (2004). The authors stated that three independent lines expressing a *CaMV35S::MIOX4* construct had an up to threefold elevated ascorbic acid content in foliar tissue. We have conducted experiments comprising wild type plants, the same *MIOX* overexpressing plants, our *miox1/2/4/5*-mutant and *vtc1* plants with a published content of ~30% of wild type ascorbic acid levels (Conklin et al. 1997), serving as a control. We measured their intrinsic foliar ascorbate under standard growth conditions and monitored it while feeding excess inositol (this data is shown in Suppl. Fig. S4) and during application of light stress (Suppl. Fig. S3c). Under all conditions tested, neither the *MIOX* overexpressing line(s) (L2 is shown representatively) nor the *miox1/2/4/5*-mutant with only marginal MIOX activity deviated significantly from wild type levels. Only the *vtc1* mutant defective in the mannose-pathway leading to ascorbic acid showed the expected decreased content.

We also performed analysis of starch and soluble sugar content in adult leaf tissue, indicating that the central

carbon metabolism is not affected in *miox1/2/4/5*-mutant or L2 MIOX overexpressor plants, since starch, glucose and sucrose levels are the same as in the wild type (data is shown in Suppl. Fig. S5).

Discussion

The analysis of *miox1/2/4/5*-mutant with a knockdown in all four *MIOX* genes clearly shows a drastic reduction of *myo*-inositol conversion into cell wall polymers and, thus, confirms the contribution to UDP-GlcA biosynthesis. Initial feeding experiments of labelled *myo*-inositol (~ 1 μM) in otherwise inositol-free MS-medium clearly showed a strong reduction of label incorporation into cell wall polymers. The low amount of *myo*-inositol in conjunction with the observed rapid metabolism of it (Endres and Tenhaken 2009), minimizes the perturbation of the *myo*-inositol pool and, thus, indicates that under normal growth conditions of seedlings and leaf discs part of the *myo*-inositol is converted into cell wall precursors. The functionality of the MIOX pathway is also supported by the better growth of wild type seedlings on regular MS-medium (containing 0.1 g L^{-1} *myo*-inositol) compared to *miox1/2/4/5*-mutant, which is further enhanced on *myo*-inositol fortified media (1 g L^{-1}). We conclude that inositol liberated from phytate degradation during seedling germination can efficiently be used for cell wall biosynthesis in the growing wild type seedling. The prerequisite for a contribution of the MIOX pathway to cell wall biosynthesis is, however, a sufficient supply of *myo*-inositol.

The *myo*-inositol pool is likely controlled by the biosynthesis and by the degradation rate. The strong increase in *myo*-inositol in *miox1/2/4/5*-mutant suggests an important role of the degradation pathway for controlling cellular inositol concentration. Smart and Flores (1997) showed a fourfold higher inositol concentration in Arabidopsis plants after overexpression of an inositol-3-phosphate synthase gene from *Spirodela polyrrhiza* under the control of the strong CaMV35S-promoter. Our *miox1/2/4/5*-mutant shows increased *myo*-inositol concentrations, though preliminary microarray experiments suggest that at least one of the three genes for *myo*-inositol biosynthesis (inositol-3-phosphate synthase; EC 5.5.1.4) is down-regulated, whereas the two others show no change in gene expression. This prompted us to look for correlated expression between the genes for inositol-3-phosphate synthases and MIOX using expression data from public databases with the Genevestigator tool (http://www.genevestigator.com). To our surprise, most tissues show no co-regulation of the two groups of genes, which we would have expected for a functional MIOX pathway for cell wall precursor biosynthesis. This suggests us that one important function of MIOX is a major contribution to balance *myo*-inositol concentrations in plant cells. Controlled levels of *myo*-inositol are also important in animal systems. Changes in *myo*-inositol concentration have been linked to common diseases. Nascimento et al. (2006), for instance, found an important cell protective role of *myo*-inositol for endothelial cells in diabetes.

MIOX role for ascorbic acid

The contribution of the MIOX-derived glucuronic acid to ascorbate biosynthesis was recently suggested by two studies, in which either the *MIOX4* gene (Lorence et al. 2004) or a purple acid phosphatase (Zhang et al. 2008) was overexpressed. We found no change in ascorbate concentration in our loss of function *miox1/2/4/5*-mutant under ambient, high light or inositol-feeding conditions. The gain of function *MIOX4* overexpressor line has an increased MIOX enzyme activity but also no increase in ascorbate concentration (Endres and Tenhaken 2009). Therefore, the role of MIOX for ascorbate in plants in analogy to the mammalian pathway is questionable. However, the possibility remains that the subsequent glucuronokinase is the channeling enzyme which guides glucuronic acid into cell wall precursors and thus prevents the conceivable conversion into ascorbate.

Metabolic consequences of MIOX loss

The *miox1/2/4/5*-mutant has elevated levels of *myo*-inositol and galactinol. This increase in galactinol in unstressed plants supports a model that the availability of *myo*-inositol is more important for galactinol biosynthesis than an increase in galactinol-synthase. Similar findings were reported for low phytate mutants from barley with increased galactinol levels, which correlates with the metabolite *myo*-inositol but not with the activity of galactinol-synthase (Karner et al. 2004).

The elevated concentration of galactinol results in an increase of the RFOs, which are typical abiotic stress-associated metabolites in plants.

Whereas Zuther et al. (2004) found no enhanced freezing/drought tolerance in plants with elevated RFO-levels, others like Taji et al. (2002) functionally linked the increased RFOs with membrane stabilization and drought or increased tolerance to reactive oxygen species (Nishizawa et al. 2008). We carefully repeated many of these experiments with the *miox1/2/4/5*-mutant and found no significant increase in freezing or paraquat (methylviologen) mediated ROS tolerance. This let us conclude that additional other unidentified metabolic changes contribute to the observed increase in stress tolerance of high level RFO-plants which may be absent in *miox1/2/4/5*-mutant.

MIOX interaction with the UGD-pathway

Surprising to us, the almost total loss in MIOX activity causes no morphological changes. The cell wall and seed mucilage composition remain similar in *miox1/2/4/5*-mutant and wild type plants. This is most likely explained by two factors: first, the limited flux of carbohydrates for cell wall precursors via the MIOX pathway in many developmental stages. These genetic data support precursor feeding studies in Arabidopsis cell cultures as reported by Sharples and Fry (2007). Second, the observed upregulation of *UGD*-genes in the *miox1/2/4/5*-mutant, which are 1.5- to 3-fold more expressed in *miox1/2/4/5*-mutant as in wild type plants, depending on the tissue. Interestingly, a reduction of UGD-activity causes strong morphological changes which are not compensated by enhanced MIOX activity (data not shown). This suggests a model that the concentration of the metabolite UDP-GlcA, or another UDP-sugar derived from it, might be a signal for *UGD* gene regulation but is of marginal influence on *MIOX* gene expression. Some hints for such a mode of regulation come from previous studies, which showed a strong gene expression of *UGD::GUS* reporter genes in etiolated seedlings, which is almost absent in light grown seedlings. A similar observation was made in developing leaves, in which stomata cells and basal cells surrounding epidermal trichomes show transient *UGD::GUS* expression during cell wall thickening.

A possible role for MIOX in pollen tube growth

MIOX genes are most prominently expressed in flowers, in particular in pollen. In former studies, Kroh and Loewus (1968) showed by feeding experiments that most of the pectin in Lily pollen cell walls was derived from the MIOX pathway. We were therefore surprised to find no reduced fertility in *miox1/2/4/5*-mutant. Obviously the remaining $\sim$10% activity (in sum) of all MIOX isoforms is sufficient to allow proper pollen development and growth. Using light microscopy we could not detect visible differences. Sections of embedded pollen were stained with monoclonal antibodies directed against different pectic epitopes (LM5, LM6, Jim5 Jim7) but failed to reveal differences between the *miox1/2/4/5*-mutant and wild type. In contrast, a knockout in UDP-sugar pyrophosphorylase as the final enzyme of the MIOX pathway to UDP-GlcA is lethal during pollen development (Schnurr et al. 2006).

It will be interesting to find out whether a stronger knockdown of residual *MIOX* genes will also cause pollen abortion. Alternatively, the UDP-sugar pyrophosphorylase has an additional function beside the activation of GlcA-1-P to UDP-GlcA. To test this we will express artifical miRNAs targeted against *MIOX* genes in the *miox1/2/4/5*-mutant background. A further but long-term approach might be required to isolate better knockout alleles and restart the crossing process.

In summary the strong knockdown of the *MIOX* gene family does not lead to visible phenotypes in Arabidopsis or to changes in the composition of the cell wall. The main pathway for UDP-GlcA as important cell wall precursor, catalyzed by the enzyme UDP-glucose dehydrogenase, is upregulated in *miox1/2/4/5* and likely compensates for the loss of MIOX activity. MIOX is responsible for *myo*-inositol breakdown and therefore involved in the homeostasis of this metabolite. The *miox1/2/4/5* mutant shows an increase in *myo*-inositol and metabolites containing *myo*-inositol.

Acknowledgments We like to thank Craig L. Nessler, Department of Plant Pathology, Virginia Tech, Blacksburg, VA, USA, for providing the *CaMV35S::MIOX* line and Mark Stitt, Max Planck Institute for Molecular Plant Physiology, Golm, Germany, for the *pgm* mutant. We are grateful to Doris Wittmann for excellent technical help. We also thank Claudia Geserick and Rebecca Reboul for fruitful discussions. The project was funded by the German Research Foundation (DFG; Te 221/6-2) and by the Austrian science fund (FWF; P20297-B16).

Conflict of interest The authors declare that they have no conflict of interest.

References

Bentsink L, Alonso-Blanco C, Vreugdenhil D, Tesnier K, Groot SP, Koornneef M (2000) Genetic analysis of seed-soluble oligosaccharides in relation to seed storability of Arabidopsis. Plant Physiol 124:1595–1604

Blackman SA, Obendorf RL, Leopold AC (1992) Maturation proteins and sugars in desiccation tolerance of developing soybean seeds. Plant Physiol 100:225–230

Brown PM, Caradoc-Davies TT, Dickson JM, Cooper GJ, Loomes KM, Baker EN (2006) Crystal structure of a substrate complex of *myo*-inositol oxygenase, a di-iron oxygenase with a key role in inositol metabolism. Proc Natl Acad Sci USA 103:15032–15037

Conklin PL, Pallanca JE, Last RL, Smirnoff N (1997) L-ascorbic acid metabolism in the ascorbate-deficient Arabidopsis mutant vtc1. Plant Physiol 115:1277–1285

Endres S, Tenhaken R (2009) *myo*-inositol oxygenase controls the level of *myo*-inositol in Arabidopsis, but does not increase ascorbic acid. Plant Physiol 149:1042–1049

Kanter U, Becker M, Friauf E, Tenhaken R (2003) Purification, characterization and functional cloning of inositol oxygenase from *Cryptococcus*. Yeast 20:1317–1329

Kanter U, Usadel B, Guerineau F, Li Y, Pauly M, Tenhaken R (2005) The inositol oxygenase gene family of Arabidopsis is involved in

the biosynthesis of nucleotide sugar precursors for cell-wall matrix polysaccharides. Planta 221:243–254
Kaplan F, Kopka J, Haskell DW, Zhao W, Schiller KC, Gatzke N, Sung DY, Guy CL (2004) Exploring the temperature-stress metabolome of Arabidopsis. Plant Physiol 136:4159–4168
Karner U, Peterbauer T, Raboy V, Jones DA, Hedley CL, Richter A (2004) *myo*-Inositol and sucrose concentrations affect the accumulation of raffinose family oligosaccharides in seeds. J Exp Bot 55:1981–1987
Klinghammer M, Tenhaken R (2007) Genome-wide analysis of the UDP-glucose dehydrogenase gene family in Arabidopsis, a key enzyme for matrix polysaccharides in cell walls. J Exp Bot 58:3609–3621
Kotake T, Yamaguchi D, Ohzono H, Hojo S, Kaneko S, Ishida HK, Tsumuraya Y (2004) UDP-sugar pyrophosphorylase with broad substrate specificity toward various monosaccharide 1-phosphates from pea sprouts. J Biol Chem 279:45728–45736
Kroh M, Loewus F (1968) Biosynthesis of pectic substance in germinating pollen: labeling with *myo*-inositol-2-14C. Science 160:1352–1354
Loewus FA, Murthy PPN (2000) *myo*-inositol metabolism in plants. Plant Sci 150:1–19
Lorence A, Chevone BI, Mendes P, Nessler CL (2004) *myo*-inositol oxygenase offers a possible entry point into plant ascorbate biosynthesis. Plant Physiol 134:1200–1205
Moskala R, Reddy CC, Minard RD, Hamilton GA (1981) An oxygen-18 tracer investigation of the mechanism of *myo*-inositol oxygenase. Biochem Biophys Res Commun 99:107–113
Nascimento NR, Lessa LM, Kerntopf MR, Sousa CM, Alves RS, Queiroz MG, Price J, Heimark DB, Larner J, Du X, Brownlee M, Gow A, Davis C, Fonteles MC (2006) Inositols prevent and reverse endothelial dysfunction in diabetic rat and rabbit vasculature metabolically and by scavenging superoxide. Proc Natl Acad Sci USA 103:218–223
Nishizawa A, Yabuta Y, Shigeoka S (2008) Galactinol and raffinose constitute a novel function to protect plants from oxidative damage. Plant Physiol 147:1251–1263
Peters S, Mundree SG, Thomson JA, Farrant JM, Keller F (2007) Protection mechanisms in the resurrection plant *Xerophyta viscosa* (Baker): both sucrose and raffinose family oligosaccharides (RFOs) accumulate in leaves in response to water deficit. J Exp Bot 58:1947–1956
Pieslinger AM, Hoepflinger MC, Tenhaken R (2010) Cloning of glucuronokinase from *Arabidopsis thaliana*, the last missing enzyme of the *myo*-inositol oxygenase pathway to nucleotide sugars. J Biol Chem 285:2902–2910
Raboy V (2001) Seeds for a better future: 'low phytate' grains help to overcome malnutrition and reduce pollution. Trends Plant Sci 6:458–462
Reiter WD (2008) Biochemical genetics of nucleotide sugar interconversion reactions. Curr Opin Plant Biol 11:236–243
Rohde P, Hincha DK, Heyer AG (2004) Heterosis in the freezing tolerance of crosses between two *Arabidopsis thaliana* accessions (Columbia-0 and C24) that show differences in non-acclimated and acclimated freezing tolerance. Plant J 38:790–799
Schneider S, Schneidereit A, Konrad KR, Hajirezaei MR, Gramann M, Hedrich R, Sauer N (2006) Arabidopsis INOSITOL TRANSPORTER4 mediates high-affinity H^+ symport of *myo*-inositol across the plasma membrane. Plant Physiol 141:565–577
Schnurr JA, Storey KK, Jung HJ, Somers DA, Gronwald JW (2006) UDP-sugar pyrophosphorylase is essential for pollen development in Arabidopsis. Planta 224:520–532
Seifert GJ (2004) Nucleotide sugar interconversions and cell wall biosynthesis: how to bring the inside to the outside. Curr Opin Plant Biol 7:277–284
Sharples SC, Fry SC (2007) Radioisotope ratios discriminate between competing pathways of cell wall polysaccharide and RNA biosynthesis in living plant cells. Plant J 52:252–262
Siddique S, Endres S, Atkins JM, Szakasits D, Wieczorek K, Hofmann J, Blaukopf C, Urwin PE, Tenhaken R, Grundler FM, Kreil DP, Bohlmann H (2009) *Myo*-inositol oxygenase genes are involved in the development of syncytia induced by *Heterodera schachtii* in Arabidopsis roots. New Phytol 184:457–472
Smart CC, Flores S (1997) Overexpression of D-*myo*-inositol-3-phosphate synthase leads to elevated levels of inositol in Arabidopsis. Plant Mol Biol 33:811–820
Taji T, Ohsumi C, Iuchi S, Seki M, Kasuga M, Kobayashi M, Yamaguchi-Shinozaki K, Shinozaki K (2002) Important roles of drought- and cold-inducible genes for galactinol synthase in stress tolerance in *Arabidopsis thaliana*. Plant J 29:417–426
Talamond P, Doulbeau S, Rochette I, Guyot JP (2000) Anion-exchange high-performance liquid chromatography with conductivity detection for the analysis of phytic acid in food. J Chromatogr A 871:7–12
Wakabayashi K, Sakurai N, Kuraishi S (1989) Effects of ABA on synthesis of cell-wall polsaccharides in segments of etiolated squash hypocotyl. I. Changes in incorporation of glucose and *myo*-inositol onto cell-wall components. Plant Cell Physiol 30:99–105
Xing G, Barr EW, Diao Y, Hoffart LM, Prabhu KS, Arner RJ, Reddy CC, Krebs C, Bollinger JM Jr (2006a) Oxygen activation by a mixed-valent, diiron(II/III) cluster in the glycol cleavage reaction catalyzed by *myo*-inositol oxygenase. Biochemistry 45:5402–5412
Xing G, Diao Y, Hoffart LM, Barr EW, Prabhu KS, Arner RJ, Reddy CC, Krebs C, Bollinger JM Jr (2006b) Evidence for C–H cleavage by an iron-superoxide complex in the glycol cleavage reaction catalyzed by *myo*-inositol oxygenase. Proc Natl Acad Sci USA 103:6130–6135
Xing G, Hoffart LM, Diao Y, Prabhu KS, Arner RJ, Reddy CC, Krebs C, Bollinger JM Jr (2006c) A coupled dinuclear iron cluster that is perturbed by substrate binding in *myo*-inositol oxygenase. Biochemistry 45:5393–5401
Zablackis E, Huang J, Muller B, Darvill AG, Albersheim P (1995) Characterization of the cell-wall polysaccharides of *Arabidopsis thaliana* leaves. Plant Physiol 107:1129–1138
Zhang W, Gruszewski HA, Chevone BI, Nessler CL (2008) An Arabidopsis purple acid phosphatase with phytase activity increases foliar ascorbate. Plant Physiol 146:431–440
Zuther E, Buchel K, Hundertmark M, Stitt M, Hincha DK, Heyer AG (2004) The role of raffinose in the cold acclimation response of *Arabidopsis thaliana*. FEBS Lett 576:169–173